Supplementary information

Supplementary Figure S1 Atg16L1 forms a large complex dependent on FIP200 in DSP-treated cells.
Wild-type (WT) and FIP200 KO MEFs were cultured in regular DMEM, harvested, and incubated on ice in the presence or absence of DSP. The soluble fractions of the cell lysates were separated by size exclusion chromatography on a Superose 6 column. Each fraction was analyzed by immunoblotting (IB) with anti-Atg16L1 and anti-Atg5 antibodies. * indicates fractions of the higher molecular mass complex of Atg12—Atg5–Atg16L1.

Supplementary Figure S2 ULK1/2 are dispensable for the Atg16L1-FIP200 interaction.
WT and ULK1/2 double KO (DKO) MEFs were harvested and treated with DSP. Cell lysates were subjected to immunoprecipitation (IP) using pre-immune serum or anti-FIP200 antibodies. The resulting precipitates were examined by immunoblot analysis with the indicated antibodies.

Supplementary Figure S3 Formation of the ULK1–Atg13–FIP200 complex is not affected in Atg5 KO MEFs.
(A) WT and Atg5 KO MEFs were cultured in regular DMEM. The soluble fractions of the cell lysates were separated by size exclusion chromatography on a Superose 6 column. Each fraction was analyzed by immunoblotting with anti-ULK1, anti-Atg13, and anti-FIP200 antibodies.
(B) Cell lysates derived from WT and Atg5 KO MEFs were subjected to immunoprecipitation (IP) using pre-immune serum or anti-FIP200 antibodies. The resulting precipitates were examined by immunoblot analysis with the indicated antibodies.

Supplementary Figure S4 The FIP200-interacting domain of Atg16L1.
(A) Schematic representations of the WT and deletion mutants of Atg16L1. Human Atg16L1α (NP_060444) has an N-terminal Atg5-interacting domain (gray box), a coiled-coil domain (shaded box), and seven WD repeats (black boxes).
(B) HEK293T cells were co-transfected with the indicated constructs. Cell lysates were analyzed by immunoprecipitation (IP) using anti-FLAG antibodies. The resulting precipitates were examined by IB analysis with anti-FLAG, anti-HA, and anti-Atg5

antibodies.
(C) Amino acid alignment of *Homo sapiens* Atg16L1α (NP_060444) with *Homo sapiens* Atg16L1β (NP_110430), *Mus musculus* Atg16L1γ (NP_001192320), *Rattus norvegicus* Atg16L1 (NP_001102279), *Xenopus laevis* Atg16L1 (NP_001091437), *Danio rerio* Atg16L1 (NP_001017854), and *Homo sapiens* Atg16L2 (NP_203746). The alignment was generated using CLUSTAL W. Identical residues are indicated with filled boxes. The black line above the *Homo sapiens* Atg16L1α sequence shows the regions required for the interaction with FIP200.

Supplementary Figure S5 The Atg16L1-FIP200 interaction is independent of Rab33B and OATL1.
HEK293T cells stably expressing FLAG-Rab33B (WT), FLAG-Rab33B Q92L (QL), T7-OATL1 (WT) or T7-OATL1 R279K (RK) were harvested and treated with DSP. Cell lysates were subjected to immunoprecipitation (IP) using pre-immune serum or anti-FIP200 antibodies. The resulting precipitates were examined by immunoblot analysis with the indicated antibodies. * indicates the positions of the immunoglobulin light chains.

Supplementary Figure S6 Isolation membrane targeting of Atg16L1 mutants in HeLa cells.
HeLa cells stably expressing GFP–ULK1 were transfected with expression plasmids encoding the indicated FLAG-tagged Atg16L1 and Atg16L1 mutants. Cells were cultured in starvation medium for 1 h, fixed, and analyzed by immunofluorescence microscopy using anti-GFP and anti-FLAG antibodies. Signal color is indicated by color of typeface. Scale bars, 10 μm, and 2 μm in inset.

Supplementary Figure S7 ULK1 dots were observed under starvation condition in the presence of wortmannin.
Atg16L1 KO MEFs stably expressing GFP–ULK1 and full-length Atg16L1(1–588), Atg16L1(1–230), or Atg16L1Δ(230–300) were cultured in starvation medium in the presence of 200 nM wortmannin for 1 h. Cells were fixed and analyzed by immunofluorescence microscopy using anti-GFP and anti-Atg16L1 antibodies. Arrowheads indicate the perinuclear localization of Atg16L1(1–230). Scale bars, 10 μm, and 2 μm in inset.

METHODS

Plasmids, antibodies, and reagents

cDNAs encoding the full-length or fragments of Atg16L1α (NP_060444) and Atg101 were amplified by PCR and subcloned into p3xFLAG–CMV-10 (Sigma-Aldrich) or pCI-neo (Promega, Tokyo, Japan) together with hemagglutinin (HA) tag. cDNAs were cloned into pMRX-IP with/without SECFP (provided by Atsushi Miyawaki, Riken) to generate pMRX-IP-Atg16L1, pMRX-IP-Atg16L1(1–230), pMRX-IP-Atg16L1Δ(230–300), pMRX-IP-SECFP-Atg16L1, pMRX-IP-SECFP-Atg16L1(1–230), and pMRX-IP-SECFP-Atg16L1Δ(230–300). The following plasmids have been previously described: HA-FIP200, HA-Atg13 [1], HA-ULK1 [2], pMXs-IP GFP-LC3, and pMRX-IP GFP-ULK1 [3]. Rabbit polyclonal anti-Atg5[4], anti-Atg9A [5], anti-FIP200 [2], anti-ULK1 [2], anti-Atg13 [1] (SAB4200100; Sigma-Aldrich), anti-Atg101 [6], anti-Atg14 [7], anti-LC3 (#1) [8], anti-REDD1 (10638-1-AP; Protein Tech), and anti-p62 (PM045; MBL) antibodies, rabbit monoclonal anti-Atg16L1 (clone D6D5; Cell Signaling Technology) antibody, mouse monoclonal anti-LC3 (clone 1703; Cosmo Bio Co.), anti-Atg16L1 (clone 1F12; MBL), anti-β actin (clone AC74; Sigma-Aldrich), anti-HA (clone 16B12; Covance), and anti-FLAG (clone M2; Sigma-Aldrich) antibodies, and rat monoclonal anti-GFP antibody (clone GF090R; Nacalai Tesque) were used. For immunostaining, AlexaFluor 488-conjugated anti-rat IgG, AlexaFluor 568-conjugated anti-mouse IgG and anti-rabbit IgG, and AlexaFluor 660-conjugated anti-mouse IgG secondary antibodies (Molecular Probes) were used. Doxycycline hydrochloride (Dox) and wortmannin were purchased from Sigma-Aldrich. Bafilomycin A_1 was purchased from Wako. Dithiobis[succinimidyl propionate] (DSP) was purchased from Thermo Scientific.

Yeast two-hybrid analysis

The yeast two-hybrid screen was performed by the Yeast Model Systems Genomics Group at Duke University using a GAL4-based two-hybrid system. Briefly, full-length mouse Atg16L1 (β isoform) was cloned into pDBLeu (Invitrogen) and transformed into AH109 cells along with the Clontech mouse brain cDNA library. Thirty-three LacZ-positive colonies were picked for isolation of DNA and 26 were found to contain sequences aligning to FIP200 encoding the region in Fig. 1A. A representative cDNA fragment encoding amino acids 1173–1413 was retested by transformation into yeast with the original bait plasmid or with empty vector followed by selection for growth on

trp-/leu- plates, followed by trp-/leu-/his-/3 mM 3-AT plates to test for growth.

Cell culture and transfection

Atg5 KO MEFs [9], Atg16L1 KO MEFs [10], FIP200 KO MEFs [11], m5-7 cells [8], HeLa cells expressing GFP-ULK1 [12] and ULK1/2 DKO MEFs [13] were generated previously. *Atg14*$^{flox/flox}$ MEFs were obtained from *Atg14*$^{flox/flox}$ mouse embryos (Saitoh et al. unpublished data), and immortalized with SV40 large T antigen using pEF321-T (a gift from Dr. Sumio Sugano). To obtain *Atg14*$^{\Delta/\Delta}$ MEFs, *Atg14*$^{flox/flox}$ MEFs were transfected with pCre-Pac in order to express the Cre recombinase transiently and cultured in the presence of puromycin [14]. The removal of the flox alleles and the absence of Atg14 protein expression were confirmed by PCR and immunoblotting, respectively. The cells stably expressing Atg16L1, Atg16L1(1–230), Atg16L1Δ(230–300), CFP-Atg16L1, CFP-Atg16L1(1–230), CFP-Atg16L1Δ(230–300), and GFP-ULK1 were generated as follows: HEK293T cells were transiently transfected using Lipofectamine 2000 (Invitrogen) reagent with the indicated plasmid together with pCG-VSV-G and pCG-gag-pol to render retroviruses infectious to human cells. WT, FIP200 KO, and Atg16L1 KO MEFs were also transfected using the indicated retrovirus. Cells were cultured in DMEM supplemented with 10% fetal bovine serum (FBS) in a 5% CO_2 incubator. For starvation treatment, cells were washed twice with PBS and incubated in amino acid-free DMEM without FBS (starvation medium).

Immunoprecipitation and immunoblotting

For immunoprecipitation analysis, HEK293T cells were transiently transfected using Lipofectamine 2000 reagent with the indicated plasmids. The cells were collected in ice-cold PBS by scraping and precipitated by centrifugation at 5000 x *g* for 3 min; precipitated cells were suspended in lysis buffer containing CHAPS (50 mM Tris-HCl, pH 7.5, 150 mM NaCl, 1 mM EDTA, 0.3% CHAPS, 0.4 mM Na_3VO_4, 10 mM NaF, 10 mM sodium pyrophosphate, 1 mM phenylmethanesulfonyl fluoride, and a protease inhibitor cocktail (Complete EDTA-free protease inhibitor, Roche)). Cell lysates were clarified by centrifugation at 12,000 x *g* for 20 min and then analyzed by immunoprecipitation using anti-FLAG M2 affinity gel (50% slurry, Sigma-Aldrich) or specific antibodies in combination with protein A or G-Sepharose (GE Healthcare). Precipitated immunocomplexes were washed five times in lysis buffer and boiled in sample buffer (46.7 mM Tris HCl, pH 6.8, 5% glycerol, 1.67% sodium dodecyl sulfate, 1.55% dithiothreitol, and 0.003% bromophenol blue). After centrifugation to precipitate the beads, the supernatant fraction was used for subsequent experiments. For

immunoblotting analysis, cells were lysed with lysis buffer containing Triton X-100. Samples were subsequently separated by SDS-PAGE and transferred to Immobilon-P polyvinylidene difluoride membranes (Millipore). Immunoblot analysis was performed with the indicated antibodies and visualized with Super-Signal West Pico Chemiluminescent substrate (Pierce Chemical Co.) or Immobilon Western Chemiluminescent HRP substrate (Millipore). To reduce the detection of immunoglobulin, Rabbit IgG Trueblot (eBioscience) or anti-rabbit peroxidase-conjugated immunoglobulin (clone RG-16; Sigma-Aldrich) was used as the secondary antibody. Signal intensities were analyzed using a LAS-3000mini imaging analyzer and Multi Gauge software version 3.0 (Fujifilm, Tokyo, Japan). Contrast and brightness adjustment was applied to the images using Photoshop 7.0.1 (Adobe Systems).

Chemical crosslinking

Cells were harvested, resuspended in ice-cold PBS containing 1 mM of DSP and incubated on ice for 30 min. The reaction was stopped by adding stop solution containing 25 mM Tris HCl. Cell lysates were analyzed by immunoprecipitation or gel filtration analysis. For immunoprecipitation analysis, lysis buffer containing 1% Triton X-100 was used.

Gel filtration analysis

Cells were homogenized in hypotonic buffer (40 mM Tris HCl, pH 7.5, and a protease inhibitor cocktail) by repeated passage (15 times) through a 1-ml syringe with a 27-gauge needle. The homogenates were centrifuged at 13,000 x *g* for 15 min, and the supernatants were further centrifuged at 100,000 x *g* 60 min. The supernatant fraction was then applied to a Superose 6 column (GE Healthcare) and eluted at a flow rate of 0.5 ml/min with elution buffer (40 mM Tris HCl, pH 7.5, and 150 mM NaCl). Fractions (0.5 ml) were then analyzed by immunoblotting. The column was calibrated with thyroglobulin (669 kDa), ferritin (440 kDa), catalase (232 kDa), albumin (67 kDa), ovalbumin (43 kDa), and cytochrome *c* (12.5 kDa).

Quantitative RT-PCR analysis

Total RNA from MEF cells was extracted using Isogen (Nippon Gene) and reverse-transcribed using ReverTraAce (Toyobo). PCR reactions were performed with SYBR Premix Ex Taq (Takara Bio) and were monitored by a Thermal Cycler Dice TP800 (Takara Bio). The ddCT method was employed to determine relative gene level

differences with GAPDH qPCR products used as a control. Primers used are listed below: ULK1, 5'-CCCAGCACTACGATGGAAAG-3' and 5'-CATAAAACAGGCGCAAATCC-3'; Atg13, 5'-CAGGCTCGACTTGGAGAAAA-3' and 5'-GCTTCATGGGTGACTTCTGG-3'; FIP200, 5'-ACCACGCTGACATTTGACACT-3' and 5'-CTCCATTGACCACCAGAACC-3'; Atg5, 5'-ATATGAAGGCACACCCCTGA-3' and 5'-CCAAGGAAGAGCTGAACTTGATG-3'; Atg16L1, 5'-AGGCGTTCGAGGAGATCATT-3' and 5'-TTCTGCTTGTAGTTTCTGGGTCA-3'. GAPDH, 5'-GCCAAGGTCATCCATGACAACT-3' and 5'-GAGGGGCCATCCACAGTCTT-3'.

Fluorescence microscopy

Cells grown on coverslips were fixed with 4% paraformaldehyde, permeabilized using 50 μg/ml digitonin, and then stained with specific antibodies. These cells were observed with a confocal laser microscope (FV1000D IX81; Olympus) using a 60x PlanApoN oil immersion lens (1.42 NA; Olympus). For final output, images were processed using Adobe Photoshop 7.0.1 software. The number of dots was determined as follows: dots were extracted using the top hat operation (parameter: 300 x 300 pixel area), and a binary image was created. Small dots (less than 10 x 10 pixel area) were removed using an open operation. The number of dots was counted using the integrated morphometry analysis program. False dots were removed by comparison with the original image.

FACS analysis

Cells stably expressing GFP-LC3 were cultured in the indicated medium for 6 h, harvested with 0.05% trypsine-EDTA, and washed with PBS. The cells were transferred to 1.5 ml tube (A.150MPC, Sarstedt), fixed with 4% paraformaldehyde, washed twice with PBS, and resuspended in 0.5 ml of PBS. The samples were analyzed using a FACSCalibur flow cytometer and Cell Quest software (BD Biosciences).

References

1. Hosokawa N *et al* (2009) Nutrient-dependent mTORC1 association with the

ULK1-Atg13-FIP200 complex required for autophagy. *Mol Biol Cell* **20:** 1981-1991

2. Hara T, Takamura A, Kishi C, Iemura S, Natsume T, Guan JL, Mizushima N (2008) FIP200, a ULK-interacting protein, is required for autophagosome formation in mammalian cells. *J Cell Biol* **181:** 497-510
3. Itakura E, Mizushima N (2010) Characterization of autophagosome formation site by a hierarchical analysis of mammalian Atg proteins. *Autophagy* **6:** 764-776
4. Mizushima N, Yamamoto A, Hatano M, Kobayashi Y, Kabeya Y, Suzuki K, Tokuhisa T, Ohsumi Y, Yoshimori T (2001) Dissection of autophagosome formation using Apg5-deficient mouse embryonic stem cells. *J Cell Biol* **152:** 657-667
5. Itakura E, Kishi-Itakura C, Koyama-Honda I, Mizushima N (2012) Structures containing Atg9A and the ULK1 complex independently target depolarized mitochondria at initial stages of Parkin-mediated mitophagy. *J Cell Sci* **125:** 1488-1499
6. Hosokawa N, Sasaki T, Iemura S, Natsume T, Hara T, Mizushima N (2009) Atg101, a novel mammalian autophagy protein interacting with Atg13. *Autophagy* **5:** 973-979
7. Itakura E, Kishi C, Inoue K, Mizushima N (2008) Beclin 1 forms two distinct phosphatidylinositol 3-kinase complexes with mammalian Atg14 and UVRAG. *Mol Biol Cell* **19:** 5360-5372
8. Hosokawa N, Hara Y, Mizushima N (2006) Generation of cell lines with tetracycline-regulated autophagy and a role for autophagy in controlling cell size. *FEBS Lett* **580:** 2623-2629
9. Kuma A, Hatano M, Matsui M, Yamamoto A, Nakaya H, Yoshimori T, Ohsumi Y, Tokuhisa T, Mizushima N (2004) The role of autophagy during the early neonatal starvation period. *Nature* **432:** 1032-1036
10. Saitoh T *et al* (2008) Loss of the autophagy protein Atg16L1 enhances endotoxin-induced IL-1β production. *Nature* **456:** 264-268
11. Gan B, Peng X, Nagy T, Alcaraz A, Gu H, Guan JL (2006) Role of FIP200 in cardiac and liver development and its regulation of TNFα and TSC–mTOR signaling pathways. *J Cell Biol* **175:** 121-133
12. Velikkakath AK, Nishimura T, Oita E, Ishihara N, Mizushima N (2012) Mammalian Atg2 proteins are essential for autophagosome formation and important for regulation of size and distribution of lipid droplets. *Mol Biol Cell*

23: 896-909

13. McAlpine F, Williamson LE, Tooze SA, Chan EYW (2013) Regulation of nutrient-sensitive autophagy by uncoordinated 51-like kinases 1 and 2. *Autophagy* **9:** in press

14. Taniguchi M, Sanbo M, Watanabe S, Naruse I, Mishina M, Yagi T (1998) Efficient production of Cre-mediated site-directed recombinants through the utilization of the puromycin resistance gene, pac: a transient gene-integration marker for ES cells. *Nucleic Acids Res* **26:** 679-680

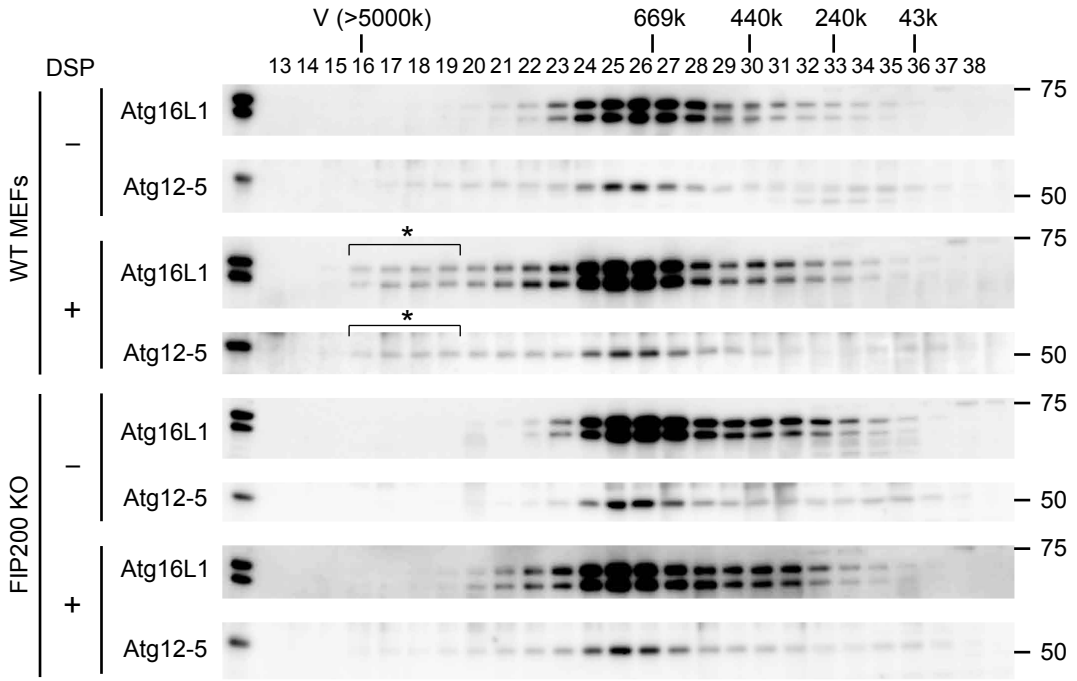

Figure S1 Nishimura et al.

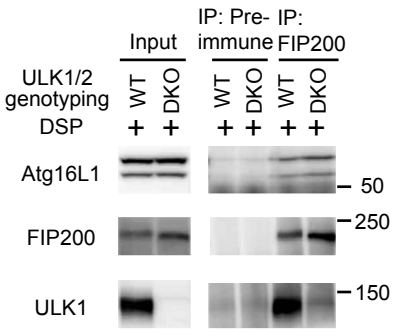

Figure S2 Nishimura et al.

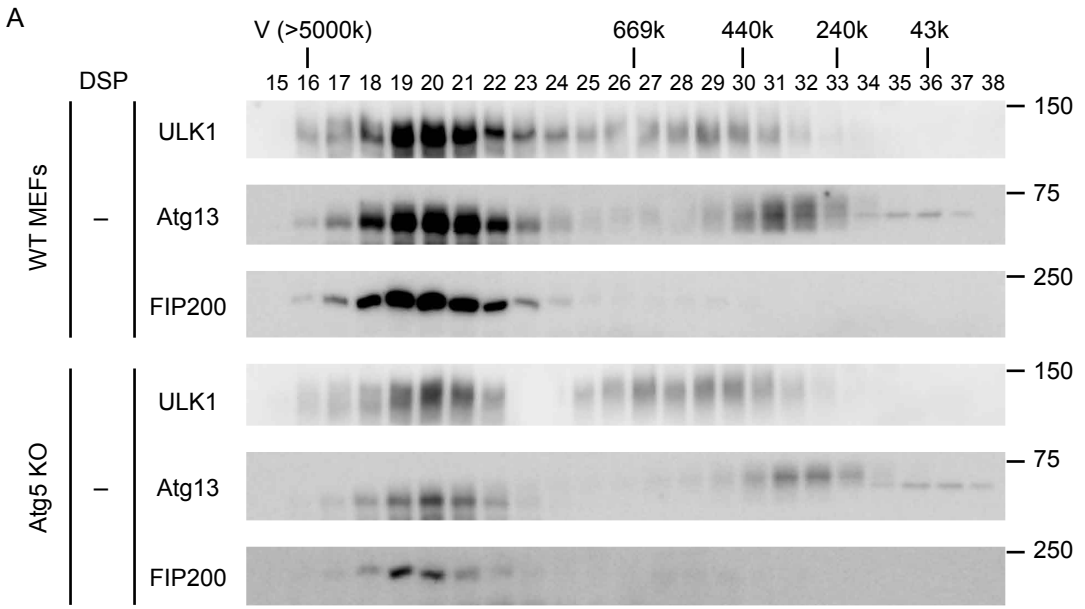

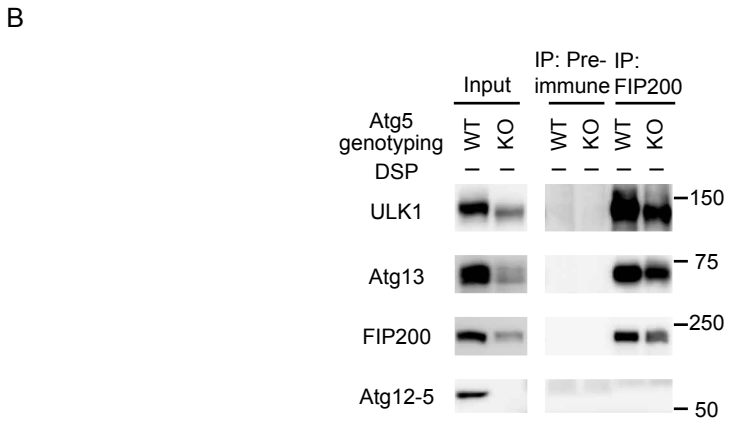

Figure S3 Nishimura et al.

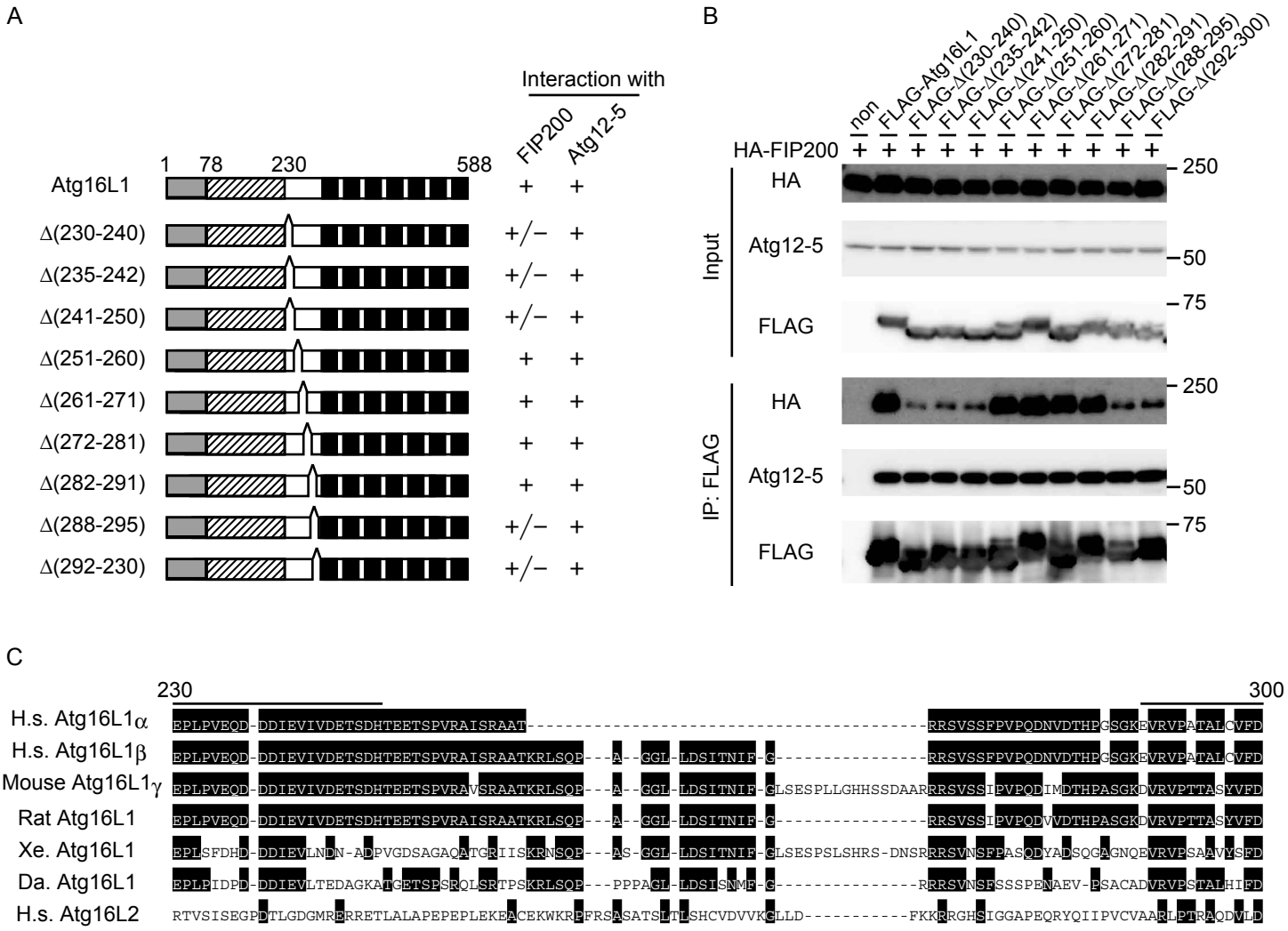

Figure S4 Nishimura et al.

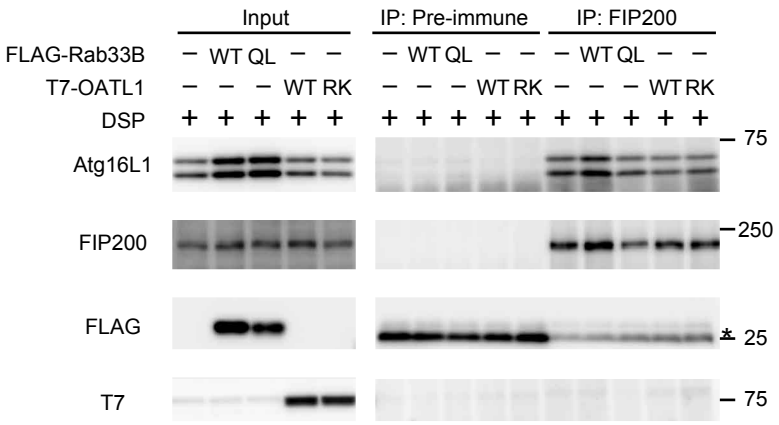

Figure S5 Nishimura et al.

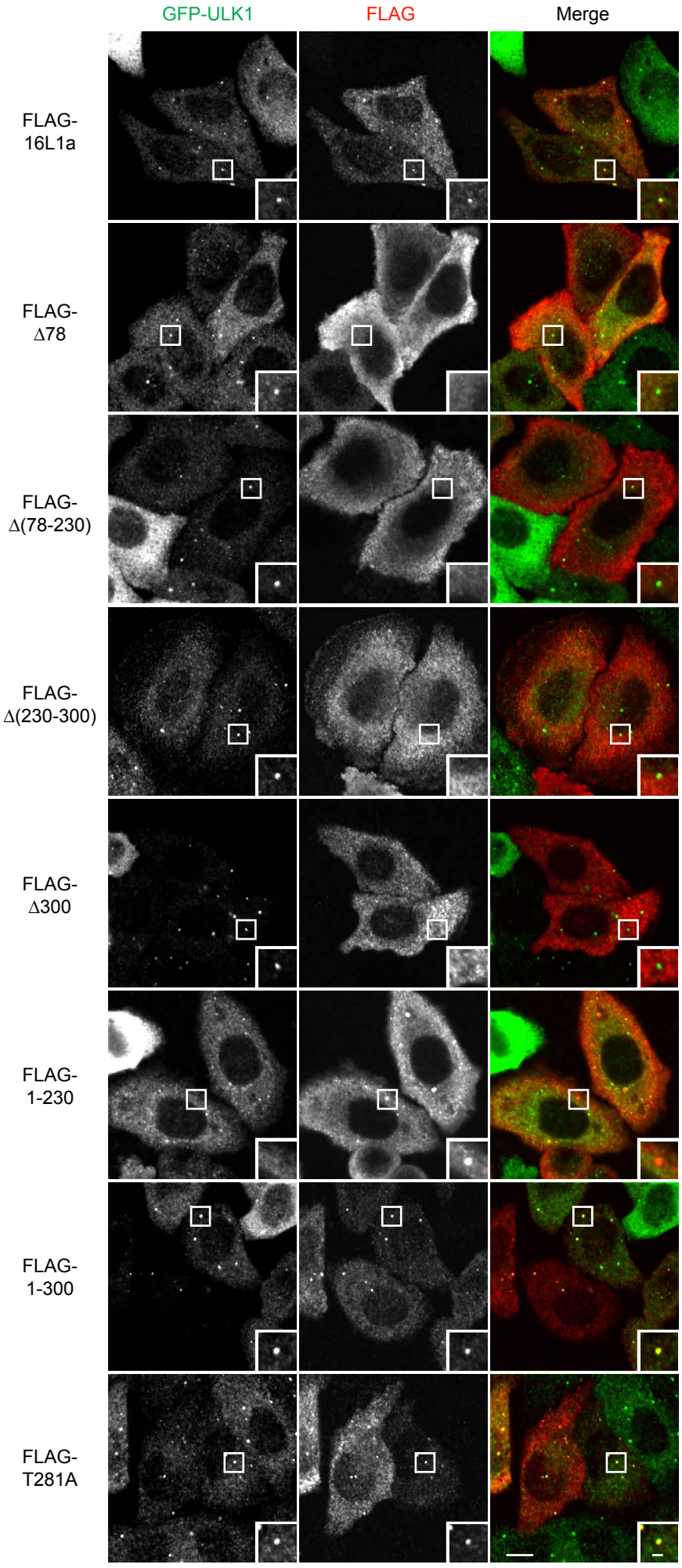

Figure S6 Nishimura et al.

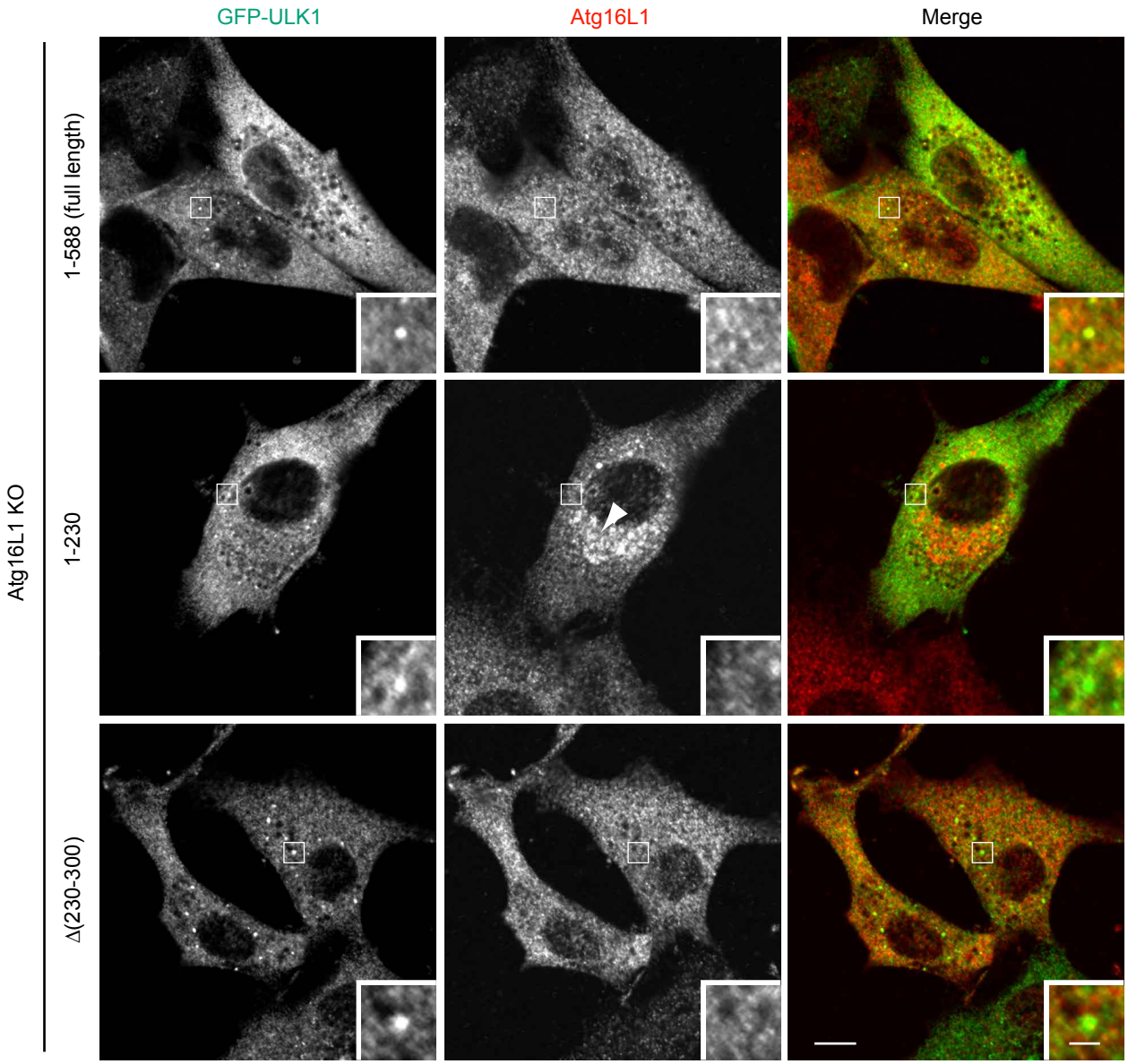

Figure S7 Nishimura et al.